Neurochemical Research (2019) 44:1950–1963
https://doi.org/10.1007/s11064-019-02829-x

ORIGINAL PAPER

UPLC-QTOF/MS-Based Metabolomics Reveals the Protective Mechanism of Hydrogen on Mice with Ischemic Stroke

Lilin Chen[1] · Yufan Chao[2] · Pengchao Cheng[1] · Na Li[2] · Hongnan Zheng[3] · Yajuan Yang[4]

Received: 4 January 2019 / Revised: 11 May 2019 / Accepted: 11 June 2019 / Published online: 24 June 2019

Abstract

As a reductive gas, hydrogen plays an antioxidant role by selectively scavenging oxygen free radicals. It has been reported that hydrogen has protective effects against nerve damage caused by ischemia–reperfusion in stroke, but the specific mechanism is still unclear. Therefore, this study aims to investigate the protective effects of hydrogen on stroke-induced ischemia–reperfusion injury and its detailed mechanism. Two weeks after the inhalation of high concentrations (66.7%) of hydrogen, middle cerebral artery occlusion (MCAO) was induced in mice using the thread occlusion technique to establish an animal model of the focal cerebral ischemia–reperfusion. Then, a metabolomics analysis of mouse cerebral cortex tissues was first performed by ultra-performance liquid chromatography-quadrupole time-of-flight mass spectrometry (UPLC-QTOF/MS) to study the metabolic changes and protective mechanisms of hydrogen on stroke ischemia–reperfusion injury. According to the metabolomic profiling of cortex tissues, 29 different endogenous metabolites were screened, including palmitoyl-L-carnitine, citric acid, glutathione, taurine, acetyl-L-carnitine, N-acetylaspartylglutamic acid (NAAG), L-aspartic acid, lysophosphatidylcholine (LysoPC) and lysophosphatidylethanolamine (LysoPE). Through pathway analysis, the metabolic pathways were concentrate on the glutathione pathway and the taurine pathway, mitochondrial energy metabolism and phospholipid metabolism that related to the oxidative stress process. This result reveals that hydrogen may protect against ischemic stroke by reducing oxidative stress during ischemia–reperfusion, thereby protecting nerve cells from reactive oxygen species(ROS).

Keywords Ischemic stroke · Metabolomics · Hydrogen · Oxidative stress · UPLC-QTOF/MS

Abbreviations

ACN	Acetonitrile
GSH-Px	Glutathione peroxidase
GSH	Glutathione
GSSG	Oxidized glutathione
H2S	Hydrogen sulphide
ISO	Isoprenaline
LysoPC	Lysophosphatidylcholine
LysoPE	Lysophosphatidylethanolamine
LPA	Lysophosphatidic acid
LysoPLD	Lysophospholipase D
MCAO	Middle cerebral artery occlusion
MDA	Malondialdehyde
NAAG	N-acetylaspartylglutamic acid
PCA	Principal component analysis
PLS-DA	Partial least squares discriminant analysis
PE	Phosphatidylethanolamine
PD	Parkinson's disease
QC	Quality control
ROS	Reactive oxygen species
SOD	Superoxide dismutase

Electronic supplementary material The online version of this article (https://doi.org/10.1007/s11064-019-02829-x) contains supplementary material, which is available to authorized users.

Lilin Chen, Yufan Chao, and Pengchao Cheng have contributed equally to this work.

✉ Hongnan Zheng
422856837@qq.com

✉ Yajuan Yang
yangyj1965@126.com

[1] College of Basic Medicine, Second Military Medical University, Shanghai 200433, People's Republic of China

[2] School of Pharmacy, Second Military Medical University, Shanghai 200433, People's Republic of China

[3] Department of Natural Medicine, School of Pharmacy, Fourth Military Medical University, Xi'an 710032, Shaanxi, People's Republic of China

[4] Department of Nursing, Changzheng Hospital, Second Military Medical University, Shanghai 200003, People's Republic of China

TTC	2,3,5-triphenyltetrazolium chloride
TCA	Citric acid cycle
VIP	Variable importance

Introduction

Stroke is a cerebrovascular accident due to a circulation disorder of the blood in the brain, which results in neurological deficit syndrome [1]. As a common refractory disease that seriously endangers human health and life safety, stroke often leads to death. The survivors of stroke may suffer from long-term disability, including paralysis and the loss of advanced cognitive functions, which gives the patient a great deal of pain and becomes a heavy burden on society and on the family [2]. According to different pathogeneses, strokes can be divided into two types: ischemic stroke and hemorrhagic stroke. Approximately 87% of strokes are caused by ischemia [3]. In treating ischemic stroke, there is no effective way to truly reverse the damage done to nerve cells by the pathophysiological mechanism [4]. Excessive production of ROS after ischemic stroke results in DNA fragmentation, lipid peroxidation, inactivation of proteins, and cell death [5]. Therefore, scavenging oxygen free radicals may be an effective treatment for ischemic stroke. Hydrogen is a colorless and odorless reductive gas that can selectively reduce the hydroxyl radical, which is the most cytotoxic of the reactive oxygen species, to effectively protect nerve cells. Japanese scientist Ohsawa proved that hydrogen can selectively reduce hydroxyl radicals and peroxynitrite in vitro and create an antioxidant effect [6]. Furthermore, hydrogen has been demonstrated to provide protection against the neuroprotection of oxidative stress-induced damage in neurological diseases, such as Parkinson's disease, Alzheimer's disease, transient and permanent cerebral ischemia and spinal cord injury [7, 8].Therefore, as a novel and effective antioxidant, hydrogen is a potential treatment for ischemic stroke.

In most studies, the concentration of hydrogen is usually no more than 4% due to safety concerns. In recent years, a new hydrogen generator which can produce 66.7% hydrogen and 33.3% oxygen by electrolyzing water was developed by the Asclepius Company. With a specific technique, it may avoid the risk for explosion of hydrogen at this high concentration. Some research groups employed high concentration hydrogen (HCH) (67% hydrogen and 33% oxygen) in the treatment of several diseases in animal models, and its protective effects were confirmed. [9–12] At present, the focus of hydrogen research is as a means of treating acute stroke. Besides, the protective effect of hydrogen pretreatment against disease have also been reported by some scientists [13–15]. We hypothesized that taken pretreatment strategy also can play a positive protective role in ischemic stroke. In our experiment, it was observed that the inhalation of high concentrations of hydrogen (66%) as a pretreatment strategy has protective effects against ischemic stroke and improve neurological outcomes. It indicated that for some high-risk groups of stroke, hydrogen pretreatment may even improve the prognosis. However, the specific mechanism of hydrogen intervention remains unclear. The severe oxidative stress to nerve damage during ischemic stroke is achieved by interfering with a series of metabolic activities in the body. Under the attack of oxygen free radicals, many abnormal metabolic activities are bound to occur in cells. After hydrogen scavenges oxygen free radicals, the metabolic abnormalities in cells are alleviated or even corrected. Therefore, analyzing the changes of metabolic pathways in this process has become a feasible way to study the intervention mechanism of hydrogen. With the development of "omics" technologies, the advantages of metabolomics as a top-down system biological approach in analyzing the changes of metabolite profiles have been increasingly realized, offering an opportunity to capture changes in the metabolic pathways in vivo, during bodily illness or other causes [16]. Metabolomics, as a downstream of proteomics, can reflect the changes more rapidly and more directly in phenotypes of individuals [17]. Cortical tissue as the target organ could be directly damaged by the mouse MCAO model, the changes in its metabolic profile can more directly reveal the abnormalities of metabolic regulation in ischemic stroke and hydrogen intervention. Therefore, we decided to analyze the mechanism of hydrogen intervention by using the UPLC-QTOF/MS platform to explore endogenous metabolites and metabolic pathway changes in stroke mice. According to changes in endogenous metabolites in the cortical tissue after hydrogen intervention, the protective mechanism of hydrogen intervention to ischemic stroke was revealed, and the relationship between metabolic pathway changes and oxidative stress in the process of hydrogen intervention was further studied.

Materials and Methods

Chemicals and Reagents

HPLC-grade acetonitrile (ACN) and methanol were purchased from Merck (Darmstadt, Germany). Formic acid and the internal standard 4-chloro-3-phenyl-L-alanine were obtained from Sigma-Aldrich (St. Louis, MO, USA). Ultrapure water was prepared using a Milli-Q water purification system (Millipore, Bedford, MA, USA). The mixed gas consisting of 67% H2 and 33% O2 was produced by the AMS-H-01 hydrogen oxygen nebulizer (Asclepius, Shanghai, China), which was specifically designed to extract the hydrogen and oxygen from water [11].

Experimental Procedure

All animal studies were performed in accordance with the National Institutes of Health (NIH) guide for the Care and Use of Laboratory Animals. All of the experimental procedures were approved by the animal experimental ethics committee of the Second Military Medical University (Shanghai, China). Forty-two male mice (20–25 g) were purchased from Shanghai Laboratory Animal Co. Ltd. (Shanghai, China) and were maintained in a humidity- and temperature-controlled animal room which was kept at approximately 50% humidity and 22 ± 2 °C under a 12 h light cycle. After conditional housing for one week, the mice were randomly divided into three groups: the control group (sham group, n = 14), the focal cerebral ischemia group (model group, n = 14) and the hydrogen intervention group (H2 group, n = 14). To establish the model of ischemic stroke, we used the middle cerebral artery occlusion (MCAO) method proposed by Zea Lona et al. [18]. To establish a hydrogen intervention model, we kept the mice in a 66.7% hydrogen atmosphere for 30 min in per day; and after 14 days of the cycle, the mice were handled with the thread embolization method. In model group, the right internal carotid artery was occluded for 2 h, then the monofilament suture was removed followed by reperfusion. In the sham group, the main procedures were the same, except there was no thread insertion.

After the operation, the ambient temperature was maintained at 25–30 °C, and the mice were put into cages for the further observation of the neurological functional deficiency scores. Neurological scoring at 24-h after reperfusion, neurological function was scored in a blind manner. The higher the score, the more serious the animal behavior disorder was [18].

Sample Collection

At 24 h after reperfusion, mice were sacrificed and the brain was collected. Mice were anesthetized by an intraperitoneal injection of 3% chloral hydrate (10 ml/kg), and the brains were quickly extracted. After stripping away the cortical tissue and placing it on ice, the eight fresh mouse brain cortices were immediately frozen in liquid nitrogen and stored at − 80 °C for biochemical and metabolomic analysis. Three brain tissue samples from each group were placed in 4% paraformaldehyde, and these were used for the preparation of pathological HE stained sections. In addition, three fresh brain tissue samples per group were used for 2,3,5-triphenyltetrazolium chloride (TTC) staining after freezing at − 20 °C for 20 min.

Brain Tissue TTC Staining and Biochemical Analysis

After removing the olfactory bulb, cerebellum and lower brainstem, the frozen brain tissue was sliced from the anterior to posterior coronal plane into six even slices, and each slice was approximately 2 mm. Brain tissue slices were placed in glass containing a 1% TTC solution. The brain tissue slices were immersed in TTC solution and stained in a constant temperature incubator at 37 °C. Each side was stained for 15 min. The stained brain slices were placed in a 4% polyformaldehyde solution for 4 h. The fixed sections of brain tissue were arranged from front to back and were scanned with a scanner. The area of cerebral infarction was calculated using ImageJ 1.41 (Wayne Rasband, National Institutes of Health, USA).

After 24-h reperfusion period, eight tissue samples of right cerebral cortex were collected from each group for biochemical detection. The levels of malondialdehyde (MDA) was tested by the method of thiobarbituric acid colorimetry, the enzymatic activities of superoxide dismutase (SOD) by the method of xanthine oxidase and glutathione peroxidase (GSH-Px) by the method of chemical colorimetry. The colorimetric kit was purchased from Nanjing Jiancheng Bio. Ins. (Nanjing, China) and an absorbance test was performed using an EPOCH enzyme labelling instrument.

Sample Preparation

After 24-h reperfusion period, eight tissue samples of right cerebral cortex from each group were weighed precisely and a 300 μL internal standard of 5 μg/mL methanol solution was added to each sample. The samples were homogenized at 60 Hz for 90 s. After 5 min at room temperature, the resulting solution mixture was spun at 13,000 rpm for 15 min at 4 °C. The clear supernatant was transferred to a sampling vial for UPLC-QTOF/MS analysis. Meanwhile, 30 μL aliquot of each cortical sample was mixed as a quality control (QC) to monitor the stability of the system and the method.

Chromatography-Mass Spectrometry Analysis

UPLC-QTOF/MS analysis was performed with an Agilent 1290 Infinity ultra-high-performance liquid chromatography equipped with an Agilent 6538 Accurate Mass Quadrupole Time-of-Flight mass spectrometer (Agilent, USA). ACQUITY UPLC HSS T3 column (2.1 mm × 100 mm, 2.5 micron, Waters, Milford, MA) that was used for chromatographic separation. The mobile phase consisted of 0.1% formic acid (A) and ACN containing 0.1% formic acid (B). The gradient eluted conditions were: 0–2 min, 5% B; 2–13 min, 5–95% B; 13–15 min, 95% B, and the post time

was 5 min for column equilibration. The column temperature was 40 °C, the flow rate was 400 µL/min, and the injection volume was 4 µL.

Positive and negative ion mode acquisition was performed using electrospray ionization mass spectrometry. The mass spectrometric parameters are as follows: the capillary voltage is 4 kV in positive mode and 3.5 kV in the negative mode; dry gas nitrogen flow rate was 11 L/min; capillary temperature was 350 °C; the spray pressure was 45 psig; the fragment voltage and skimmer voltage were set at 120 and 60 V. The acquisition range was set at 100–1100 m/z. The 121.0509 and 922.0098 m/z in positive mode and 112.985587 and 1033.988109 m/z in negative mode were selected as the internal standard ion for real-time mass correction.

Data Processing and Statistical Analysis

Agilent MassHunter workstation software version B.01.04 (Agilent, MA, USA) was operated to acquire and process all data. First, the UPLC-MS raw data (.d) were converted into a common data format (.mzdata) files. The threshold of the absolute peak height was set to 500. Then, XCMS and R software were used to extract and match the peaks to generate a visual data matrix. Finally, principal component analysis (PCA) and supervised partial least squares discriminant analysis (PLS-DA) were performed with the SIMCA-P software after 80% principle screening and internal standard normalization.

SPSS 21.0 software was used to analyze the data of the sham group, model group and hydrogen intervention group. The difference is considered significant when the ANOVA value is less than 0.05, and the P is less than 0.05. MetaboAnalyst (http://www.metaboanalyst.ca) and KEGG (https://www.kegg.jp) were used for the enrichment analysis of metabolic pathways.

Results

Behavioral and Biochemical Analysis

The neurological functional deficiency score was mainly used to assess the neurological status of mice. The higher the score, the more serious the neurological impairment and the worse the dysfunction. By observing the behavior of three groups of mice, the neurobehavioral score was evaluated. The neurobehavioral score results of each group are shown in Table 1. The specific behavioral score of each mouse is shown in Supplemental Table 1. The score of the sham group was 0, which indicated that the nerve function was intact, and there was no disturbance of activity. The score of the H_2 group was significantly lower than that of model group ($P < 0.001$), which indicated that the nerve function of H_2 group was recovered to a certain extent, and the brain injury was reduced.

Table 1 Neurobehavioral scores of mice in three groups (Mean ± SD)

Group	Numbers (n)	Behavioral scores
Sham group	14	0
Model group	14	3.29 ± 0.61
H_2 group	14	2.00 ± 0.65[a]

$P < 0.001$

[a]Compared with the model group

As shown in Fig. 1, the brain cells in the sham group were arranged in order, stained uniformly without bleeding, swelling and injury, inflammatory cell infiltration or vasodilation (Fig. 1a). In contrast, the model group showed hemorrhage in the brain tissue and vasodilation around the hemorrhagic focus, showing inflammatory cell infiltration (Fig. 1b). After intervention with hydrogen, the astrocyte edema and inflammatory cell infiltration in the brain tissue of mice were significantly reduced, the area of haemorrhagic focus was decreased (Fig. 1c), suggesting that the degree of cerebral ischemia in the H_2 group was lower than that in the model group, hydrogen reduced the ischemic injury and the hemorrhagic transformation after MCAO.

After staining with 1% TTC solution, the normal brain tissue was red, while the infarct focus was pale. The brain tissue of the normal group was dark red after TTC staining, and no white staining (Fig. 1d) was found. In the model group, large white areas were found in the brain tissues, which were ischemic stroke necrosis tissues (Fig. 1e). After hydrogen intervention, the white area of brain tissue was significantly smaller than that in model group (Fig. 1f), which indicated that the cerebral infarction injury in the H_2 group was significantly lower than that in model group. The area of cerebral infarction in the three groups was significantly different (Fig. 1 g), which suggested that hydrogen has a protective effect on ischemic stroke.

SOD and GSH-Px are the most important antioxidant enzymes in organisms, and their enzymatic activities changes represent the antioxidant state of organisms. Compared to the sham group, the activities of SOD and GSH-Px decreased significantly ($P < 0.001$) in the model group, the activities of SOD and GSH-Px increased significantly ($P < 0.01$) in H2 group (Fig. 2a, b). As a decomposition product of lipid peroxidation, the content of MDA indirectly reflects the level of free radical metabolism in

organisms and the severity of free radical attack on cells. In the H2 group, a significant reduction of MDA levels comparing to the model group ($P < 0.05$) was observed (Fig. 2c).

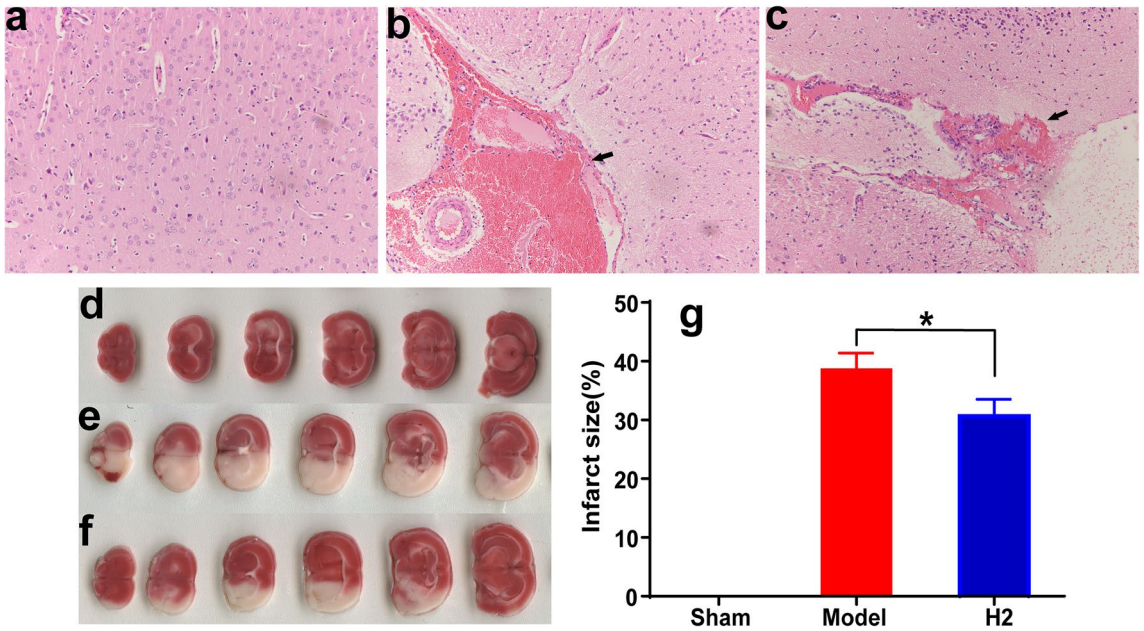

Fig. 1 Staining results of the brain tissue sections. **a** A normal section of brain from the sham group; **b** A pathological section of brain from the model group, with obvious hemorrhagic foci; **c** A pathological section of brain from the hydrogen intervention group, in which the hemorrhagic foci were significantly smaller than those in model group; **d** TCC-stained brain section from the sham group, which is shown by a normal red color; **e** TCC-stained section from the model group, with large white hemorrhagic foci; **f** TCC-stained section from the H2 group, in which the white necrotic tissue was significantly reduced; **g** Cerebral infarction area in the sham operation group, the model group and the hydrogen intervention group. The area of white necrotic tissue was zero in the sham group; and compared to the model group; the area of white necrotic tissue decreased significantly in the H2 group. *P < 0.05, H2 group compared to the model group; the statistical results are expressed by the mean ± SD

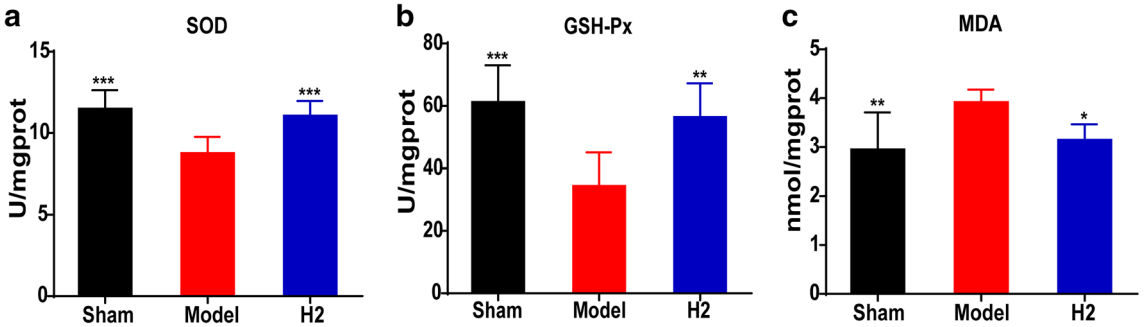

Fig. 2 Detection of the oxidative index in the cerebral cortex. **a** The enzymatic activities of SOD in the sham group, the model group and the H2 group. Compared to the model group, enzymatic activities of SOD in the H2 group was increased; **b** The enzymatic activities of GSH-Px in the sham group, the model group and the H2 group. Compared to the model group, the enzymatic activities of GSF-Px in the H2 group showed a significant rebound; **c** The level of MDA in sham group, the model group and the H2 group. Compared to the model group, the level of MDA in the H2 group decreased significantly. *P < 0.05, **P < 0.01, ***P < 0.001, compared to the model group

Cortical Metabolomics Analysis

Data acquisition based on UPLC-QTOF/MS in positive and negative ion modes showed that the QC samples had good overlap (Fig. 3), thereby indicating that the instrument was stable during the operation of the sequence, and the representative total ion chromatograms (Supplemental Fig. 1) of each group showed that the peaks were in good shape and dispersed from each other. It shows that the experimental method is suitable for the cortical sample test.

Through multivariate statistical analysis, unsupervised PCA analysis was used to assess the correlation of samples and to select outliers. Samples from the sham group have a distinct trend of dispersion with samples from the model group and the hydrogen intervention group, and the degree of aggregation of the QC samples was well (Supplemental

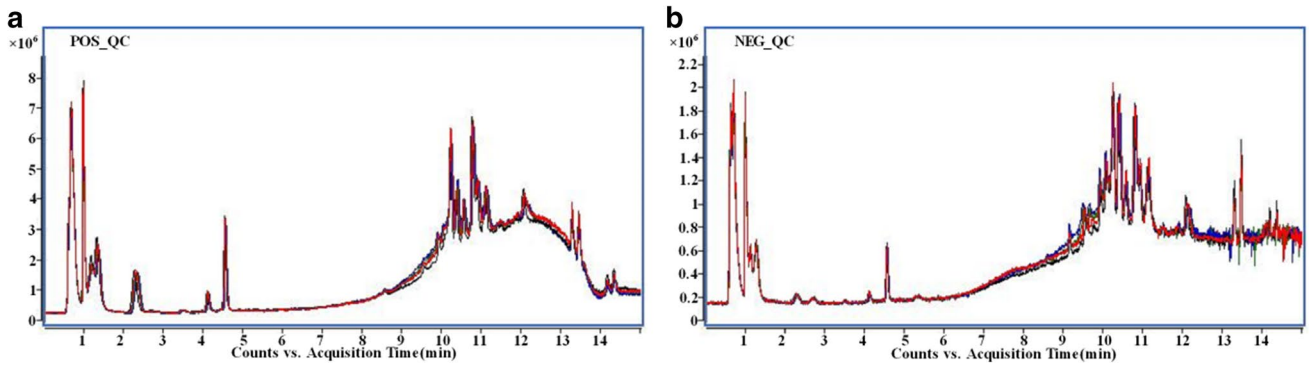

Fig. 3 The total ion chromatograms of the QC sample. **a** The total ion chromatograms superposition diagram of the QC sample in positive mode; **b** The total ion chromatograms superposition diagram of the QC sample in negative mode

Fig. 2a, b). The difference between the three groups was significant, which indicated that the cerebral cortex of the model and the H_2 groups had significant changes in metabolite level compared to the sham group.

PLS-DA analysis was used to analyze the metabolic profiles of the three groups of samples.

The PLS-DA score plots of both positive and negative modes showed significant dispersion of the three groups of samples, and the hydrogen intervention group showed a significant regression trend (Supplemental Fig. 2c, d) compared to the model group. To screen out the different metabolites in the three groups, PLS-DA analysis was performed separately between the sham group and the model group. From the PLS-DA score plots in positive and negative mode, it can be seen that there is a significant separation trend between the two groups (Fig. 4a, b), and the scatter plots (Fig. 4c, d) showed that the distance of the variable from the origin contributes to the difference between the sample groups, with a larger variable importance (VIP) value, the farther the variable. In addition, the PLS-DA model was tested for fit using the permutation test, and the results showed that the model did not show any overfitting phenomenon (Fig. 4e, f) under either positive or negative modes. In this experiment, the variable VIP > 1.0 was regarded as a possible differential metabolite, and all data of the sham group, model group and hydrogen intervention group were analyzed by one-way ANOVA and the Tukey test. Finally, VIP > 1 and $P < 0.05$ were determined to be the screening criteria for differential metabolites.

In this study, 29 metabolites (Table 2), such as palmitoylcarnitine, citric acid, glutathione, taurine, acetyl-levo-carnitine, N-acetylaspartate glutamic acid, N-acetylasparagine, N-acetylaspartate, aspartate, lysophosphatidylcholines [such as LysoPC (18:0), LysoPC (0:0/20:4)] and lysophosphatidylethanolamines [such as LysoPE (0:0/20:4) and LysoPE (0:0/18:2)] were identified by searching Metlin (http://metlin.scripps.edu/) and HMDB (http://www.hmdb.ca/) online databases based on the mass–charge ratio (m/z) and retention time. Cluster analysis of differential metabolites revealed their relative changes in the three groups in the form of heat maps (Fig. 5).

Discussion

Protective Mechanisms of Hydrogen on Mice with Ischemic Stroke

In this study, we investigated the protective effects of hydrogen in mice model of ischemic stroke. MetaboAnalyst (http://www.metaboanalyst.ca) and KEGG (http://www.genome.jp/kegg) were used to analyze the metabolic pathways of these differential metabolites. The results showed that these metabolic pathways mainly focused on glutathione metabolism, taurine metabolism, mitochondrial energy metabolism, and phospholipid metabolism (Fig. 6), which were closely related to oxidative stress [19–22] and suggested that these metabolic pathways may be the protective mechanisms of hydrogen on ischemic stroke. These results were also consistent with brain sensitivity to oxidative stress because of characteristics such as high oxygen consumption rate, rich transition metal and unsaturated lipids with strong redox ability, and low availability of antioxidant enzymes. Therefore, we analyzed the oxidative stress of the brain from the level of the metabolic pathway to reveal the possible protective mechanism of hydrogen on the MCAO stroke mice.

Glutathione Metabolism and Oxidative Stress

Glutathione is a core substance in glutathione metabolism. It is rich in sulfhydryl (–SH) and is widely distributed in various organs of the body. It plays an important role in maintaining cell biological function, and this is no exception in nerve cells [23]. Under oxidative stress conditions, GSH is

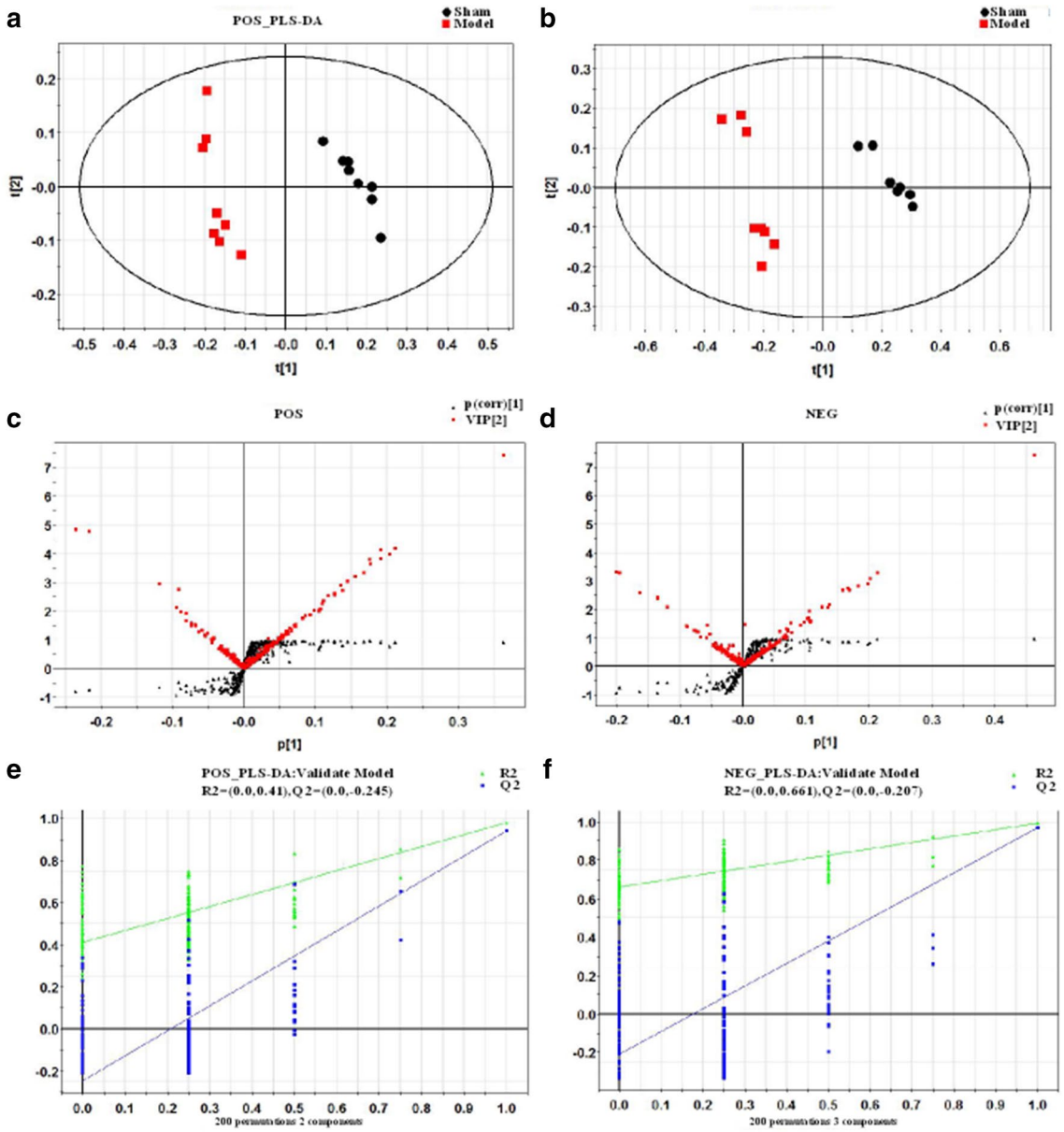

Fig. 4 PLS-DA analysis of the sham group and the model group. **a** The PLS-DA score plot of the sham group and the model group in positive mode, showing a good separation trend; **b** The PLS-DA score plot of the sham group and the model group in negative mode, showing a good separation trend; **c** The scatter plot in the positive mode; **d** The scatter plot of in the negative mode; **e** The permutation test of the sham group and the model group in the positive mode, showing that the model was a good fit; **f** The permutation test of the sham group and the model group under negative mode

oxidized to GSSG, and the ratio of GSH/GSSG is decreased. GSH is an important antioxidant in the body. Its main physiological function is to scavenge free radicals in the human body and protect sulfhydryl groups in many proteins and enzymes [24, 25]. In addition, a common limiting factor for reduced glutathione synthesis is the bioavailability of intracellular cysteine. Because extracellular cysteine is easily oxidized to cystine, maintaining the reduction state of extracellular cysteine is beneficial to the synthesis of reduced glutathione [26]. Iyer et al. found that inducing the extracellular oxidation of cysteines to cystine leads to decreased GSH content [27]. While intracellular H_2S reduces cystine to cysteine, cysteine can be easily introduced into cells and used for GSH production [28]. Like hydrogen sulfide (H2S), hydrogen is also a small molecule strong reductive gas that can enter and exit cells freely and has a similar effect to hydrogen sulfide. Therefore, the MCAO model in this study caused a decrease in glutathione content due to oxidative stress, and the GSH content was recovered after inhaling a higher concentration of hydrogen. We considered that

Table 2 List of differential metabolites in cortical samples from H_2 group

No.	m/z	Ion	Metabolites	Formula	VIP[a]	P[b]	FC[c]
1	72.0810	$[M+H]^+$	Pyrrolidine	C4H9N	1.07	0.0000	1.03
2	124.0079	$[M-H]^-$	Taurine	C2H7NO3S	1.11	0.0362	1.20
3	134.0446	$[M+H]^+$	L-Aspartic acid	C4H7NO4	1.10	0.0000	1.10
4	160.1328	$[M+H]^+$	DL-2-Aminooctanoic acid	C8H17NO2	1.68	0.0424	0.48
5	162.0582	$[M+H]^+$	2-Indolecarboxylic acid	C9H7NO2	2.74	0.0000	1.03
6	174.0407	$[M-H]^-$	N-acetylaspartate	C6H9NO5	5.67	0.0000	1.21
	176.0551	$[M+H]^+$	N-acetylaspartate	C6H9NO5	1.67	0.0000	1.08
7	191.0198	$[M-H]^-$	Citric acid	C6H8O7	2.04	0.0110	0.82
8	204.1228	$[M+H]^+$	Acetylcarnitine	C9H17NO4	1.71	0.0000	1.65
9	303.0828	$[M-H]^-$	N-Acetylaspartylglutamic acid	C11H16N2O8	1.55	0.0340	1.11
10	306.0766	$[M-H]^-$	Glutathione	C10H17N3O6S	2.20	0.0000	1.90
	308.0910	$[M+H]^+$	Glutathione	C10H17N3O6S	3.20	0.0000	1.79
11	400.3416	$[M+H]^+$	Palmitoyl-L-carnitine	C23H45NO4	1.35	0.0006	0.86
12	427.0706	$[M+H]^+$	Urolithin A-3-*O*-glucuronide	C19H16O10	1.65	0.0431	2.49
13	436.2832	$[M-H]^-$	PE (P-16:0)	C21H44NO6P	1.70	0.0000	1.18
	438.2974	$[M+H]^+$	PE (P-16:0)	C21H44NO6P	1.40	0.0000	1.24
14	466.3285	$[M+H]^+$	PE (P-18:0)	C23H48NO6P	1.39	0.0000	1.50
15	471.0619	$[M-H]^-$	Fumarprotocetraric acid	C22H16O12	2.73	0.0473	2.74
16	478.2941	$[M-H]^-$	LysoPE (0:0/18:1)	C23H46NO7P	1.56	0.0092	0.99
	480.3082	$[M+H]^+$	LysoPE (0:0/18:1)	C23H46NO7P	4.99	0.0000	0.85
17	480.3094	$[M-H]^-$	LysoPE (18:0)	C23H48NO7P	2.59	0.0000	1.12
	482.3237	$[M+H]^+$	LysoPE (18:0)	C23H48NO7P	2.99	0.0000	1.34
18	494.3237	$[M+H]^+$	LysoPC (16:1)	C24H48NO7P	1.32	0.0000	1.13
19	496.3394	$[M+H]^+$	LysoPC (16:0)	C24H50NO7P	1.54	0.0079	1.00
	540.3308	$[M+FA-H]^-$	LysoPC (16:0)	C24H50NO7P	2.51	0.0000	1.13
20	500.2785	$[M-H]^-$	LysoPE (0:0/20:4)	C25H44NO7P	2.75	0.0000	1.13
21	522.2835	$[M+FA-H]^-$	LysoPE (0:0/18:2)	C23H44NO7P	1.36	0.0000	1.04
22	524.2976	$[M+H]^+$	LysoPS (18:1)	C24H46NO9P	3.35	0.0000	2.12
23	524.3706	$[M+H]^+$	LysoPC (18:0)	C26H54NO7P	4.03	0.0000	1.20
	546.3523	$[M+Na]^+$	LysoPC (18:0)	C26H54NO7P	1.01	0.0000	1.35
	568.3617	$[M+FA-H]^-$	LysoPC (18:0)	C26H54NO7P	1.96	0.0000	1.16
24	526.2934	$[M-H]^-$	LysoPE (0:0/22:5)	C27H46NO7P	1.00	0.0304	1.79
25	528.3095	$[M-H]^-$	LysoPE (0:0/22:4)	C27H48NO7P	2.98	0.0000	1.23
26	544.3397	$[M+H]^+$	LysoPC (0:0/20:4)	C28H50NO7P	2.55	0.0227	1.28
27	556.3392	$[M+Na]^+$	LysoPE (0:0/22:2)	C27H52NO7P	1.12	0.0000	1.64
28	558.3547	$[M+Na]^+$	LysoPE (22:1)	C27H54NO7P	1.18	0.0000	1.56
29	611.1445	$[M-H]^-$	Oxidized glutathione	C20H32N6O12S2	1.12	0.0001	1.57

[a]VIP values of variables in sham group and model group

[b]P values of variables in sham group and model group

[c]FC value of variables in H_2 group and the model group

hydrogen can selectively scavenge hydroxyl radicals to reduce GSH consumption [29]; and hydrogen increases the availability of cysteine to increases the production of GSH. Armstrong et al. found that the decrease in the GSH content is a potential early activation signal of apoptosis, and the subsequent generation of oxygen free radicals promote cell apoptosis [30]. In summary, the increase in GSH content after the inhalation of hydrogen is of great significance for the treatment of stroke.

Taurine Metabolism and Oxidative Stress

Taurine, a sulfur-containing nonprotein amino acid, which does not participate in the biosynthesis of proteins in vivo but is closely related to the metabolism of cystine and cysteine. Furthermore, it has been reported that taurine has an antioxidant activity [31] that can inhibits oxidative stress by promoting GSH biosynthesis [32] and regulate the production rate of ROS in mitochondria to combat oxidative stress

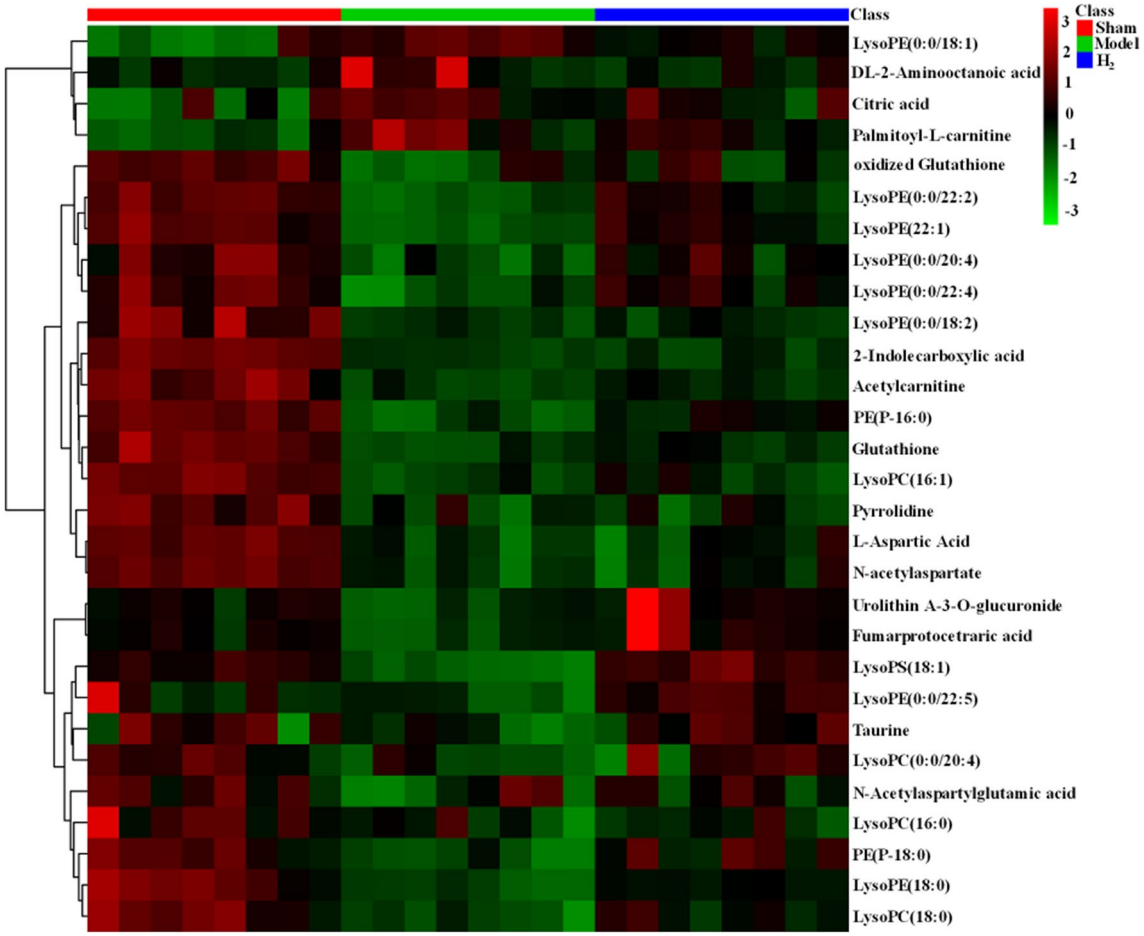

Fig. 5 Cluster analysis of 29 differential metabolites. The color depth of the heat map represents the relative intensity of the differential metabolites in the samples from the sham, model and H_2 groups

[33, 34]. Therefore, the content of taurine was increased, and the area of cerebral infarction was reduced in the hydrogen intervention group on account of reducing the consumption of taurine after inhaling hydrogen, increasing the activity of GSH-Px, and promoting the production of GSH, so that a reduction in the production of ROS alleviated the damage of oxidative stress to nerve cells. It has been reported that taurine can prevent the brain from acrylonitrile-induced lipid peroxidation [35]. In addition, it can protect the brain against Huntington's disease, Alzheimer's disease and stroke [36]. Moreover, Gharibani et al. found that taurine can reduce neurological deficits, cerebral infarct volume and caspase-3 activity in the ischemic penumbra 24 h after middle cerebral artery occlusion [36].

Mitochondrial Energy Metabolism

In this study, the citric acid in the MCAO model increased, and the citric acid in the hydrogen intervention group decreased. It may be that the aconitase was inactivated by ROS attack during a stroke, which interfered with the metabolic process of citric acid conversion to isocitrate. Selective removal of oxygen-free radicals after the inhalation of hydrogen inhibits the toxic effects of ROS on cis-aconitase, and the mitochondrial oxidation process of citric acid conversion to isocitrate continues, thereby maintaining normal energy metabolism. Because the mitochondrial respiratory chain and the steady state of the citric acid cycle (TCA) are necessary for maintaining human brain function, dysfunction can lead to energy production disorders and damage to the brain.

In the TCA cycle, citric acid is converted to isocitrate catalyzed by aconitase. The aconitase is a TCA cycle enzyme with a 4Fe–4S protein center. The [4Fe–4S] cluster has obvious sensitivity to oxidative stress, resulting in the enzyme being easily inactivated by the reactive oxygen species [37]. For example, the inactivation of mitochondrial aconitase by superoxide anion plays an important role in the pathogenesis of Parkinson's disease (PD) [38]. In addition, inhibition of aconitase results in the low flux

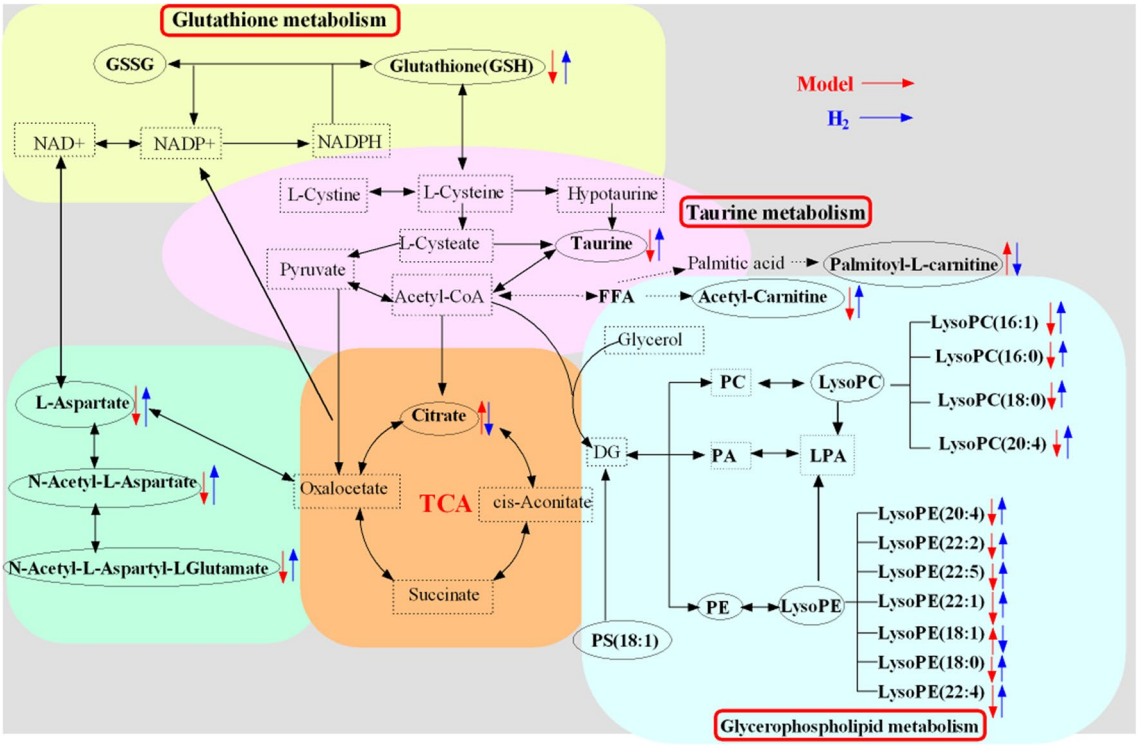

Fig. 6 The metabolic pathway networks resulting from the ischemic stroke under hydrogen intervention. Metabolites in the red arrow represent progressive elevation, or a declining trend from the model group to the sham group; metabolites in the blue arrow represent progressive elevation, or a declining trend from the H2 group to the model group

of the TCA cycle and reduces ATP production, ultimately leading to increase neuronal death [39].

In this research, acetyl-L-carnitine was downregulated, and palmitoylcarnitine was upregulated during stroke in mice, but the opposite was true after inhaling hydrogen. Changes in the polar metabolite carnitines affect mitochondrial energy metabolism. Among them, acetyl-L-carnitine is a natural form of L-carnitine, which is a short-chain carnitine that is especially rich in the muscle and in the brain, and it is involved in a series of important metabolic process in vivo [40]. Acetyl-L-carnitine can traverse the blood–brain barrier and help provide enough energy for brain cells [41]. As studies have shown, carnitine and its acyl ester are powerful antioxidants, free radical scavengers, and iron integrators [42]. Adding acetyl-L-carnitine to astrocytes prevents changes in the mitochondrial respiratory chain complex activity and antioxidant status [43]. Furthermore, the decrease of carnitine and acetylcarnitine in the process of rat I/R (ischemia/reperfusion) injury indicates that the antioxidant defense system is defective [44]. Acetyl-L-carnitine can improve antioxidant capacity. Sharman et al. [45] found that as protein oxidation in the aged brain decreased, oxidative stress decreased, and antioxidant levels increased under acetyl-L-carnitine treatment. Moreover, acetyl-L-carnitine can improve mitochondrial function and reduce membrane lipid peroxidation by regulating oxidative stress [46, 47]

Palmitoylcarnitine, as a carrier of fatty acids into mitochondria, helps fatty acids transfer into the mitochondria and can mediate the beta-oxidation of fatty acids [48]. Studies have shown that palmitoylcarnitine and palmitoyl-CoA can affect mitochondrial membrane potentials and the production of ROS [49]. Excessive Pal-car may cause an inappropriate increase in palmitoyl-CoA in the mitochondrial matrix, thereby accelerating ROS production and impairing mitochondrial function [50]. In this study, after the inhalation of hydrogen, the content of palmitoylcarnitine decreased, and the content of acetyl L-carnitine increased, thus reflecting the oxidation/antioxidative stress of carnitine.

Phospholipid Metabolism

Phospholipids, which are extremely important biological molecules in the brain, are the main components of the cell membrane and are important energy reservoirs that play a key role in cell signal transduction. Lysophospholipids are intermediates in the metabolism of phospholipids and are involved in cell membrane lysis, apoptosis, and inflammatory responses [51]. Lysophospholipids is reported to be closely related to oxidative stress [52]. In

nerve cells, lysophosphatidylcholine may further aggravate ischemia–reperfusion injury by increasing intracellular calcium overload under ischemic conditions [53]. However, studies have shown that lysophosphatidylcholines and lysophosphatidylethanolamines have protective effects on ischemic neurons [54]. During oxidative stress, phospholipase A2 will be overactivated, hydrolyzing phospholipids into lysophospholipids and various free fatty acids [55]. For example, phospholipase A2 can hydrolyze arachidonic acid at the phospholipids [such as phosphatidylcholine (16:0/20:4) and phosphatidylethanolamine (16:0/20:4)] sn-2 bit to generate free arachidonic acid and LysoPC/LysoPE (16:0/0:0). However, the contents of LysoPC [(0:0/20:4) and LysoPE (0:0/20:4)] increased in the hydrogen intervention group, which indicated that the sn-2 bond hydrolysis of phospholipids decreased, and oxidative stress was alleviated. Furthermore, in the process of oxidative stress, the unsaturated double bonds in phospholipids were easily oxidized, thus causing the peroxidation of cellular lipids [56, 57]. In this study, the content of LysoPC (0:0/20:4), LysoPE (0:0/22:2), LysoPE (0:0/20:4), LysoPE (0:0/18:2), LysoPE (0:0/22:5), and LysoPE (0:0/22:4) in the hydrogen intervention group increased, which indicated that the oxidation of unsaturated double bonds was reduced, which was also related to changes in oxidative stress-related indicators MDA and GSH-Px. Lysophosphatide can be further acylated to glycerophospholipids under the action of fatty acid coenzyme A to maintain the stability of nerve cell membranes [58]. Furthermore, lysophospholipids with different substituent groups also have different functions. In a study on the prehypertension group, elevated lysoPC (16:0) levels increased oxidative stress, thereby increasing pro-inflammatory response and arterial stiffness [59]. LysoPE, especially lysoPE (18:0) linked to ether, can elevate Ca^{2+} concentration in nerve cells through the G protein-coupled receptor pathway, thereby leading to calcium overload to induce the injury of nerve cells [60]. However, in the case of myocardial infarction induced by a high Isoprenaline (ISO) dose, the enhancement of oxidative stress observed in rat myocardium was related to the decrease of lysoPCs [LysoPC (18:0) and lysoPC (20:3)] level [61]. In addition, LysoPC, LysoPE and other phosphatidylipids can be metabolized into lysophosphatidic acid (LPA) through an autotaxin and lysoPLD; LPA are involved in a wide range of pathophysiological activities, and their metabolic changes are more significantly correlated with oxidative stress [62–64]. In summary, compared with model group, lysophosphocholines [LysoPC (16:1), LysoPC (16:0), LysoPC (18:0), LysoPC (0:0/20:4)] and lysophosphoethanolamines [LysoPE (0:0/22:2), LysoPE (22:1/0:0), LysoPE (0:0/18:0), LysoPE (0:0/20:4), LysoPE (0:0/18:2), LysoPE (0:0/22:5), and LysoPE (0:0/22:4)] increased in the hydrogen intervention group, only LysoPE(0:0/18:1) was reduced, which indicated that the process of hydrogen improved stroke has a relationship between the phospholipids metabolism and reduced oxidative stress.

NAAG and Aspartic Acid Metabolism

In this experiment, NAAG was downregulated in MCAO mice, and the NAAG content was upregulated after inhalation of hydrogen, suggesting that NAAG is associated with the protective effects of hydrogen on stroke intervention. studies have found that excessive release of glutamate after nerve injury is often accompanied by the release of another protective peptide neurotransmitter NAAG [65, 66]. High levels of glutamate release and increased Ca^{2+} flux can induce the production of reactive oxygen species and inhibit GSH synthesis [67]. NAAG is a potent agonist of the type 3 metabotropic glutamate receptor (mGluR3) and can promote astrocyte uptake of glutamate and reduce the synaptic glutamate freed [68, 69]. However, after it is released, NAAG is rapidly hydrolyzed by glutamate carboxypeptidase II on glial cells into N-acetylaspartate, thereby losing the above endogenous neuroprotective effects [70, 71]. Furthermore, studies have shown that the activation of mGluR3 helps to restore endogenous GSH levels, reduce ROS production, scavenge free radicals and stabilize the function of the mitochondria [72, 73]. Therefore, the inhalation of hydrogen may increase in NAAG content, activating mGluR3, reducing the production of reactive oxygen species and promoting GSH synthesis to reduce oxidative stress damage.

The literature reports that aspartic acid has a certain antioxidative stress effect [74]. Therefore, the change of aspartic acid content after the inhalation of hydrogen has certain significance for resisting oxidative stress damage caused by the generation of hydroxyl radicals.

Conclusions

In summary, a metabonomics approach based on UPLC/Q-TOF MS was first applied to profile the metabolic alterations of the cerebral cortices of mice with ischemic stroke under hydrogen intervention. Hydrogen intervention significantly reduced brain damage and improved the metabolic aberrations caused by stroke in mice. After analysis, the identification of a total of 29 differential metabolites that are primarily involved in the glutathione pathway and taurine pathway, as well as in mitochondrial energy metabolism and phospholipid metabolism, supported the idea that these metabolic pathways are closely related to the protective effect of hydrogen in ischemic stroke.

Acknowledgements This research was supported by the Effect of frailty assessment and multidisciplinary doctor-nurse combination intervention on outcome of postoperative prognosis in elderly patients

(No. 2018czh-z16), the key program foundation for nursing research of Changzheng Hospital, Second Military Medical University.

Data Availability The data used to support the findings of this study are available from the corresponding author upon request.

Authors' Contribution All authors contributed to this work, prepared the manuscript, and approved this version of the paper.

Compliance with Ethical Standards

Conflict of interest The authors declare that there is no conflict of interest regarding the publication of this paper.

References

1. Johnson W, Onuma O, Owolabi M, Sachdev S (2016) Stroke: a global response is needed. Bull World Health Organ 94:634–634A. https://doi.org/10.2471/BLT.16.181636
2. Patil VC, Jatal S, Rajput A, Bangar K (2015) Clinical and imaging profile of ischemic verses hemorrhagic stroke. IJHSR 5(3):49–58
3. Lyden P, Zivin J (1993) Hemorrhagic transformation after cerebral ischemia: mechanisms and incidence. Cerebrovasc Brain Metab Rev 5:1–16
4. Allen CL, Bayraktutan U (2009) Oxidative stress and its role in the pathogenesis of ischaemic stroke. Int J Stroke 4:461–470. https://doi.org/10.1111/j.1747-4949.2009.00387.x
5. Szabó C, Ischiropoulos H, Radi R (2007) Peroxynitrite: biochemistry, pathophysiology and development of therapeutics. Nat Rev Drug Discov 6:662–680
6. Fukuda K-I et al (2007) Inhalation of hydrogen gas suppresses hepatic injury caused by ischemia/reperfusion through reducing oxidative stress. Biochem Biophys Res Commun 361:670–674. https://doi.org/10.1016/j.bbrc.2007.07.088
7. Hong Y, Chen S, Zhang J-M (2010) Hydrogen as a selective antioxidant: a review of clinical and experimental studies. J Int Med Res 38:1893–1903. https://doi.org/10.1177/147323001003800602
8. Hong Y et al (2014) Neuroprotective effect of hydrogen-rich saline against neurologic damage and apoptosis in early brain injury following subarachnoid hemorrhage: possible role of the Akt/GSK3β signaling pathway. PLoS ONE 9:e96212. https://doi.org/10.1371/journal.pone.0096212
9. Huang JL, Liu WW, Sun XJ (2018) Hydrogen inhalation improves mouse neurological outcomes after cerebral ischemia/reperfusion independent of anti-necroptosis. Med Gas Res 8:1–5. https://doi.org/10.4103/2045-9912.229596
10. Jin C et al (2016) Inhalation of water electrolysis-derived hydrogen ameliorates cerebral ischemia-reperfusion injury in rats—a possible new hydrogen resource for clinical use. Neuroscience 335:232–241
11. Huang L (2016) Molecular hydrogen: a therapeutic antioxidant and beyond. Med Gas Res 6:219–222. https://doi.org/10.4103/2045-9912.196904
12. Li H et al (2017) Inhalation of high concentrations of hydrogen ameliorates liver ischemia/reperfusion injury through A2A receptor mediated PI3 K-Akt pathway. Biochem Pharmacol 130:83–92. https://doi.org/10.1016/j.bcp.2017.02.003
13. Huang L, Applegate RL 2nd, Applegate PM, Boling W, Zhang JH (2018) Inhalation of high concentration hydrogen gas improves short-term outcomes in a rat model of asphyxia induced-cardiac arrest. Med Gas Res 8:73–78. https://doi.org/10.4103/2045-9912.241063
14. Liu W et al (2013) Combined early fluid resuscitation and hydrogen inhalation attenuates lung and intestine injury. World J Gastroenterol 19:492–502. https://doi.org/10.3748/wjg.v19.i4.492
15. Zhang CB, Tang YC, Xu XJ, Guo SX, Wang HZ (2015) Hydrogen gas inhalation protects against liver ischemia/reperfusion injury by activating the NF-kappaB signaling pathway. Exp Ther Med 9:2114–2120. https://doi.org/10.3892/etm.2015.2385
16. Fiehn O (2002) Metabolomics–the link between genotypes and phenotypes. Plant Mol Biol 48:155–171
17. Su L, Zhao H, Zhang X, Lou Z, Dong X (2016) UHPLC-Q-TOF-MS based serum metabonomics revealed the metabolic perturbations of ischemic stroke and the protective effect of RKIP in rat models. Mol BioSyst 12:1831–1841. https://doi.org/10.1039/C6MB00137H
18. Longa E, Weinstein P, Carlson S, Cummins R (1989) Reversible middle cerebral artery occlusion without craniectomy in rats. Stroke 20:84–91
19. Zhou H-G et al (2013) Glutathione prevents free fatty acids-induced oxidative stress and apoptosis in human brain vascular endothelial cells through Akt pathway. CNS Neurosci Ther 19:252–261. https://doi.org/10.1111/cns.12068
20. Li Y et al (2012) Taurine attenuates methamphetamine-induced autophagy and apoptosis in PC12 cells through mTOR signaling pathway. Toxicol Lett 215:1–7. https://doi.org/10.1016/j.toxlet.2012.09.019
21. Abdel-Salam OME et al (2014) Citric acid effects on brain and liver oxidative stress in lipopolysaccharide-treated mice. J Med Food 17:588–598. https://doi.org/10.1089/jmf.2013.0065
22. Servitja J-M, Masgrau R, Pardo R, Sarri E, Picatoste F (2000) Effects of oxidative stress on phospholipid signaling in rat cultured astrocytes and brain slices. J Neurochem 75:788–794. https://doi.org/10.1046/j.1471-4159.2000.0750788.x
23. Bains JS, Shaw CA (1997) Neurodegenerative disorders in humans: the role of glutathione in oxidative stress-mediated neuronal death. Brain Res Rev 25:335–358. https://doi.org/10.1016/S0165-0173(97)00045-3
24. Shimada S et al (2016) Hydrogen gas ameliorates hepatic reperfusion injury after prolonged cold preservation in isolated perfused rat liver. Artif Organs 40:1128–1136. https://doi.org/10.1111/aor.12710
25. Samarghandian S, Azimi-Nezhad M, Farkhondeh T, Samini F (2017) Anti-oxidative effects of curcumin on immobilization-induced oxidative stress in rat brain, liver and kidney. Biomed Pharmacother Biomed Pharm 87:223–229. https://doi.org/10.1016/j.biopha.2016.12.105
26. Hurst RD, Heales SJR, Dobbie MS, Barker JE, Clark JB (1998) Decreased endothelial cell glutathione and increased sensitivity to oxidative stress in an in vitro blood–brain barrier model system. Brain Res 802:232–240. https://doi.org/10.1016/S0006-8993(98)00634-9
27. Iyer SS et al (2009) Oxidation of extracellular cysteine/cystine redox state in bleomycin-induced lung fibrosis. Am J Physiol Lung Cell Mol Physiol 296:L37–L45. https://doi.org/10.1152/ajplung.90401.2008
28. Kimura Y, Goto Y-I, Kimura H (2010) Hydrogen sulfide increases glutathione production and suppresses oxidative stress in mitochondria. Antioxid Redox Signal 12:1–13. https://doi.org/10.1089/ars.2008.2282
29. Peng Z et al (2015) Inhalation of hydrogen gas ameliorates glyoxylate-induced calcium oxalate deposition and renal oxidative stress in mice. Int J Clin Exp Pathol 8:2680–2689
30. Armstrong JS, Jones DP (2002) Glutathione depletion enforces the mitochondrial permeability transition and causes cell death in Bcl-2 overexpressing HL60 cells. FASEB J 16:1263–1265. https://doi.org/10.1096/fj.02-0097fje

31. Saransaari P, Oja S (1996) Taurine and neural cell damage. Transport of taurine in adult and developing mice. Adv Exp Med Biol 403:481–490
32. Hung C (2006) Effect of taurine on gastric oxidative stress and hemorrhagic erosion in brain ischemic rats. Chin J Physiol 49:152–159
33. Marcinkiewicz J (2010) Taurine bromamine (TauBr)—its role in immunity and new perspectives for clinical use. J Biomed Sci 17:S3–S3. https://doi.org/10.1186/1423-0127-17-S1-S3
34. Schaffer SW, Azuma J, Mozaffari M (2009) Role of antioxidant activity of taurine in diabetes. This article is one of a selection of papers from the NATO Advanced Research Workshop on Translational Knowledge for Heart Health (published in part 1 of a 2-part Special Issue). Can J Physiol Pharmacol 87:91–99. https://doi.org/10.1139/y08-110
35. Mahalakshmi K, Pushpakiran G, Anuradha CV (2003) Taurine prevents acrylonitrile-induced oxidative stress in rat brain. Pol J Pharmacol 55:1037
36. Gharibani, P. M. et al.(Year) 241-258 (Springer New York Published)
37. Zhang S-J et al (2007) Activation of aconitase in mouse fast-twitch skeletal muscle during contraction-mediated oxidative stress. Am J Physiol-Cell Physiol 293:C1154–C1159. https://doi.org/10.1152/ajpcell.00110.2007
38. Liang L-P, Patel M (2004) Iron-sulfur enzyme mediated mitochondrial superoxide toxicity in experimental Parkinson's disease. J Neurochem 90:1076–1084. https://doi.org/10.1111/j.1471-4159.2004.02567.x
39. Cantu D, Schaack J, Patel M (2009) Oxidative inactivation of mitochondrial aconitase results in iron and H(2)O(2)-mediated neurotoxicity in rat primary mesencephalic cultures. PLoS ONE 4:e7095. https://doi.org/10.1371/journal.pone.0007095
40. Thal LJ, Calvani M, Amato A, Carta A (2000) A 1-year controlled trial of acetyl-l-carnitine in early-onset AD. Neurology 55:805
41. Inano A et al (2003) Acetyl-L-carnitine permeability across the blood–brain barrier and involvement of carnitine transporter OCTN2. Biopharm Drug Dispos 24:357–365. https://doi.org/10.1002/bdd.371
42. Arduini A (1992) Carnitine and its acyl esters as secondary antioxidants? Am Heart J 123:1726–1727. https://doi.org/10.1016/0002-8703(92)90850-U
43. Calabrese V et al (2005) Acetylcarnitine induces heme oxygenase in rat astrocytes and protects against oxidative stress: involvement of the transcription factor Nrf2. J Neurosci Res 79:509–521. https://doi.org/10.1002/jnr.20386
44. Liu Y et al (2012) Metabolomic changes and protective effect of L-carnitine in rat kidney ischemia/reperfusion injury. Kidney Blood Press Res 35:373–381. https://doi.org/10.1159/000336171
45. Sharman EH, Vaziri ND, Ni Z, Sharman KG, Bondy SC (2002) Reversal of biochemical and behavioral parameters of brain aging by melatonin and acetyl l-carnitine. Brain Res 957:223–230. https://doi.org/10.1016/S0006-8993(02)03551-5
46. Poon HF, Calabrese V, Calvani M, Butterfield PDA (2006) Proteomics analyses of specific protein oxidation and protein expression in aged rat brain and its modulation by L-acetylcarnitine: insights into the mechanisms of action of this proposed therapeutic agent for CNS disorders associated with oxidative stress. Antioxid Redox Signal 8:381–394. https://doi.org/10.1089/ars.2006.8.381
47. Ribas GS, Vargas CR, Wajner M (2014) L-carnitine supplementation as a potential antioxidant therapy for inherited neurometabolic disorders. Gene 533:469–476. https://doi.org/10.1016/j.gene.2013.10.017
48. Endlicher R et al (2009) Peroxidative damage of mitochondrial respiration is substrate-dependent. Physiol Res 58:685–692
49. Tominaga H et al (2008) Different effects of palmitoyl-l-carnitine and palmitoyl-CoA on mitochondrial function in rat ventricular myocytes. Am J Physiol-Heart Circ Physiol 295:H105–H112. https://doi.org/10.1152/ajpheart.01307.2007
50. Goñi FM, Requero MA, Alonso A (1996) Palmitoylcarnitine, a surface-active metabolite. FEBS Lett 390:1–5. https://doi.org/10.1016/0014-5793(96)00603-5
51. Farooqui AA, Horrocks LA, Farooqui T (2000) Glycerophospholipids in brain: their metabolism, incorporation into membranes, functions, and involvement in neurological disorders. Chem Phys Lipid 106:1–29. https://doi.org/10.1016/S0009-3084(00)00128-6
52. Li X et al (2016) Mitochondrial reactive oxygen species mediate lysophosphatidylcholine-induced endothelial cell activation. Arterioscler Thromb Vasc Biol 36:1090–1100. https://doi.org/10.1161/ATVBAHA.115.306964
53. Farooqui AA, Horrocks LA (2006) Phospholipase A-generated lipid mediators in the brain: the good, the bad, and the ugly. The Neuroscientist 12:245–260. https://doi.org/10.1177/1073858405285923
54. Blondeau N, Lauritzen I, Widmann C, Lazdunski M, Heurteaux C (2002) A potent protective role of lysophospholipids against global cerebral ischemia and glutamate excitotoxicity in neuronal cultures. J Cereb Blood Flow Metab 22:821–834. https://doi.org/10.1097/00004647-200207000-00007
55. Martínez J, Moreno J (2001) Role of Ca2 + -independent phospholipase A2 on arachidonic acid release induced by reactive oxygen species. Arch Biochem Biophys 392:257–262. https://doi.org/10.1006/abbi.2001.2439
56. Sala P et al (2015) Determination of oxidized phosphatidylcholines by hydrophilic interaction liquid chromatography coupled to fourier transform mass spectrometry. Int J Mol Sci 16:8351–8363. https://doi.org/10.3390/ijms16048351
57. Gruber F, Bicker W, Oskolkova OV, Tschachler E, Bochkov VN (2012) A simplified procedure for semi-targeted lipidomic analysis of oxidized phosphatidylcholines induced by UVA irradiation. J Lipid Res 53:1232–1242. https://doi.org/10.1194/jlr.D025270
58. Sun GY, MacQUARRIE RA (1989) Deacylation-reacylation of arachidonoyl groups in cerebral phospholipids. Ann N Y Acad Sci 559:37–55. https://doi.org/10.1111/j.1749-6632.1989.tb22597.x
59. Kim M, Jung S, Kim SY, Lee S-H, Lee JH (2014) Prehypertension-associated elevation in circulating lysophosphatidlycholines, Lp-PLA(2) activity, and oxidative stress. PLoS ONE 9:e96735. https://doi.org/10.1371/journal.pone.0096735
60. Lee J-M, Park S-J, Im D-S (2015) Lysophosphatidylethanolamine increases intracellular Ca2 + through LPA1 in PC-12 neuronal cells. Biochem Biophys Res Commun 461:378–382. https://doi.org/10.1016/j.bbrc.2015.04.042
61. Liu Y-T et al (2013) The metabolic disturbances of isoproterenol induced myocardial infarction in rats based on a tissue targeted metabonomics. Mol BioSyst 9:2823–2834. https://doi.org/10.1039/C3MB70222G
62. Bian D et al (2006) The G12/13-RhoA signaling pathway contributes to efficient lysophosphatidic acid-stimulated cell migration. Oncogene 25:2234–2244
63. Storz P, Döppler H, Toker A (2005) Protein kinase D mediates mitochondrion-to-nucleus signaling and detoxification from mitochondrial reactive oxygen species. Mol Cell Biol 25:8520–8530. https://doi.org/10.1128/MCB.25.19.8520-8530.2005
64. García-Fernández M et al (2012) Chronic immobilization in the malpar1 knockout mice increases oxidative stress in the hippocampus. Int J Neurosci 122:583–589. https://doi.org/10.3109/00207454.2012.693998

65. Zhong C et al (2005) NAAG peptidase inhibitor reduces acute neuronal degeneration and astrocyte damage following lateral fluid percussion TBI in rats. J Neurotrauma 22:266–276. https://doi.org/10.1089/neu.2005.22.266
66. Zhong C, Luo Q, Jiang J (2014) Blockade of N-acetylaspartylglutamate peptidases: a novel protective strategy for brain injuries and neurological disorders. Int J Neurosci 124:867–873. https://doi.org/10.3109/00207454.2014.890935
67. Cao Y et al (2016) Glutamate carboxypeptidase II gene knockout attenuates oxidative stress and cortical apoptosis after traumatic brain injury. BMC Neurosci 17:15. https://doi.org/10.1186/s12868-016-0251-1
68. Yourick DL, Koenig ML, Durden AV, Long JB (2003) N-acetylaspartylglutamate and β-NAAG protect against injury induced by NMDA and hypoxia in primary spinal cord cultures. Brain Res 991:56–64. https://doi.org/10.1016/S0006-8993(03)03533-9
69. Zuo D, Bzdega T, Olszewski RT, Moffett JR, Neale JH (2012) Effects of N-acetylaspartylglutamate (NAAG) peptidase inhibition on release of glutamate and dopamine in prefrontal cortex and nucleus accumbens in phencyclidine model of schizophrenia. J Biol Chem 287:21773–21782. https://doi.org/10.1074/jbc.M112.363226
70. Yao H-H et al (2005) Enhancement of glutamate uptake mediates the neuroprotection exerted by activating group II or III metabotropic glutamate receptors on astrocytes. J Neurochem 92:948–961. https://doi.org/10.1111/j.1471-4159.2004.02937.x
71. Zhong C et al (2006) NAAG peptidase inhibitor increases dialysate NAAG and reduces glutamate, aspartate and GABA levels in the dorsal hippocampus following fluid percussion injury in the rat. J Neurochem 97:1015–1025. https://doi.org/10.1111/j.1471-4159.2006.03786.x
72. Zhou F et al (2006) Activation of Group II/III metabotropic glutamate receptors attenuates LPS-induced astroglial neurotoxicity via promoting glutamate uptake. J Neurosci Res 84:268–277. https://doi.org/10.1002/jnr.20897
73. Berent-Spillson A, Russell JW (2007) Metabotropic glutamate receptor 3 protects neurons from glucose-induced oxidative injury by increasing intracellular glutathione concentration. J Neurochem 101:342–354. https://doi.org/10.1111/j.1471-4159.2006.04373.x
74. Duan J et al (2016) Dietary supplementation with l-glutamate and l-aspartate alleviates oxidative stress in weaned piglets challenged with hydrogen peroxide. Amino Acids 48:53–64. https://doi.org/10.1007/s00726-015-2065-3